

INTERSTELLAR DUST MODELS TOWARDS SOME IUE STARS

N. KATYAL^{1,2}, R GUPTA¹, D B VAIDYA³

¹Inter University centre for Astronomy and Astrophysics, Pune, India

²School of Physical Sciences, Jawaharlal Nehru University, New Delhi 110067, India

³ICCSIR, Ahmedabad, 380006, India

(Received August 16, 2003; Revised September 17, 2003; Accepted September 30, 2003)

Accepted to PASP

ABSTRACT

We study the extinction properties of the composite dust grains, consisting of host silicate spheroids and graphite as inclusions, using discrete dipole approximation (DDA). We calculate the extinction cross sections of the composite grains in the ultraviolet spectral region, 1200Å -3200Å and study the variation in extinction as a function of the volume fraction of the inclusions. We compare the model extinction curves with the observed interstellar extinction curves obtained from the data given by the International Ultraviolet Explorer (IUE) satellite. Our results for the composite grains show a distinct variation in the extinction efficiencies with the variation in the volume fraction of the inclusions. In particular, it is found that the wavelength of peak absorption at ‘2175Å’ shifts towards the longer wavelength with the variation in the volume fraction of inclusions. We find that the composite grain models with the axial ratios viz. 1.33 and 2.0 fit the observed extinction reasonably well with a grain size distribution, $a = 0.005\text{-}0.250\mu\text{m}$. Moreover, our results of the composite grains clearly indicate that the inhomogeneity in the grain structure, composition and the surrounding media modifies the extinction properties of the grains.

Subject headings: Interstellar Dust, Extinction, Ultraviolet spectra

1. INTRODUCTION

In 1968, the first satellite, OAO2, capable of UV observations was launched. Till then, due to atmospheric extinction, the astronomical studies in the ultraviolet spectral region were not possible. Later on other satellites like TD-1, Astronomical Netherland satellite (ANS) and International Ultraviolet Explorer (IUE) were launched. IUE has provided a wealth of data on interstellar extinction in the UV region. We study the wavelength dependence of the interstellar extinction in the UV region, 1200-3200Å, observed by the IUE satellite towards several stars in the various interstellar environments; viz. diffuse interstellar medium, HII region, OB type association, reflection nebulae, dense medium and HI sources.

Recent studies of interplanetary, cometary and interstellar dust indicate that the cosmic dust grains are inhomogeneous viz. porous, fluffy and composite. The collected interplanetary particles are also porous and composite (Brownlee 1987). Mathis (1996), Dwek (1997), Li & Greenberg (1998) and Zubko et al. (2004a) have proposed composite grain models consisting of silicates and amorphous carbon to explain the observed wavelength dependence of interstellar extinction, polarization, albedo, IR emission and the observed elemental depletion. They have used the effective medium theory (EMT). Iati et al. (2004) have studied optical properties of the composite grains using the transition matrix approach. Voshchinnikov et al. (2006) and Voshchinnikov & Henning (2008) have used the layered sphere method to study the extinction properties of the porous grains. Very recently, Siebenmorgen et al. (2013) have used a dust model, consisting of a mixture of large spheroidal amorphous carbon (AMC) and silicate grains. Small grains of graphite, silicates and polycyclic aromatic hydrocarbons (PAHs) are also included to explain the ex-

tingtion, emission, linear and circular polarization in the diffuse interstellar medium. Clayton et al. (2003b) have used Maximum Entropy Method (MEM) and EMT for 2-component (silicates and graphite) and 3-component (silicates, graphite and amorphous carbon) spherical grain models to study the extinction properties in the Milky Way galaxy and the Magellanic clouds. In EMT, the inhomogeneous particle is replaced by a homogeneous one with some ‘average effective dielectric function’. The effects related to the fluctuations of the dielectric function within the inhomogeneous structure can not be treated by this approach of the EMT.

We have used Discrete Dipole Approximation (DDA) which allows consideration for irregular shape effects, surface roughness and internal structure within the grain (Wolff et al. 1994, 1998). Since there is no exact theory to study these porous and composite particles, there is a need to formulate models of electromagnetic scattering by approximate methods like EMT and DDA. We have used DDA to calculate the extinction cross sections of the composite grains in the spectral UV region, 1200Å - 3200Å, and compared the model extinction curves with the extinction curves, derived from the IUE satellite observations. For a discussion and comparison of EMT and DDA see for e.g. Ossenkopf (1991) and Wolff et al. (1998). Earlier Vaidya et al. (2001, 2007) have used composite grain models to interpret the average observed interstellar extinction. Moreover, the recent results of Katyal et al. (2011) show that the composite grain model is more efficient as compared to the bare silicate/graphite grain models in producing the extinction and also reducing the cosmic abundance constraints. Composite dust grain models are also being employed to analyze IR emission. Recently, Vaidya & Gupta (2011) have used the composite grain model to interpret the observed IR emis-

sion from circumstellar dust. Massa et al. (1983) have done spectrophotometric measurements for a sample of stars judged by Meyer & Savage (1981) to study highly anomalous peculiar UV extinction as inferred from the broad-band Astronomical Netherlands Satellite (ANS) data. These observations showed a discrete bump feature at 2175Å (Stecher 1965, 1969). This feature has been ascribed to small graphite grains (Stecher & Donn 1965; Draine & Malhotra 1993).

Other possible candidate for the spectral bump at 2175Å could be polycyclic aromatic hydrocarbons (PAHs) as discussed by Li & Draine (2001) and Mallocci et al. (2008). Siebenmorgen et al. (2013) have also discussed about the strong electronic transitions of both graphites and PAHs at 2175Å to be responsible for the bump feature. Greenberg & Chlewicki (1983) have found strong correlation between the strength of the ‘2175Å’ feature and the visible extinction. They obtained a poor correlation between far ultraviolet (FUV) extinction, strength of the feature and visible extinction concluding that a wide spectrum of size distribution is needed to explain the average observed interstellar extinction curve. Xiang et al. (2011) have shown that the carriers responsible for the 2175Å feature and the extinction in the UV might not be the same.

Wavelength dependent studies of the interstellar extinction curves are the best tool for understanding environment around these stars. The most commonly used technique for deriving the wavelength dependence of interstellar extinction is the ‘‘pair method’’ (Massa et al. 1983). Basically, the ratio of the fluxes of the reddened and comparison star gives a direct measurement of the dust extinction towards the reddened star. The resultant ratio, after normalization is referred to as the ‘extinction curve’. Errors resulting from poorly matched pairs can dominate the uncertainties of individual extinction curves. Fitzpatrick & Massa (1986, 1988, 1990) analyzed several IUE extinction curves and found that all these curves could be fitted extremely well by a single analytical expression with six parameters.

With the availability of much more observational data, revisions of earlier dust models was done as extinction of light is highly subject to the interstellar environments from where it passes through. Therefore, Clayton & Mathis (1988); Cardelli et al. (1989) (hereafter called CCM method) found that in general, the properties of UV extinction curves are correlated with the extinction in the optical/IR region and that from the UV through the IR. They characterized this dependence by a single parameter, R_v^{-1} , which is the ratio of visual extinction to total extinction of V, and is defined as $R_v = A(V)/E(B-V)$. However, the CCM method has its limitations, both from the standpoint of understanding dust grain properties and dereddening energy distributions. While the UV curve shapes indeed correlate in general with R_v , the R_v^{-1} dependence adopted by CCM is insufficient to describe the behavior over the entire range of observed R_v values, and breaks down at small R_v . Further, the CCM formula does not provide particularly good fits to individual extinction curves. Evidently, factors other than R_v , e.g. chemical composition, processing history, ambient radiant field play important roles in determining the extinction properties. Hence,

based on different interstellar environments of the stars, Aiello et al. (1988) have presented a collection of 115 extinction curves derived from low dispersion IUE spectra. The atlas includes extinction originating in the diffuse medium and several major nebulae and dense clouds. The data can be easily accessed and used for various extinction studies.

The shape of extinction curves are substantially different for different R_v 's, and hence changes in the size distributions is also expected. As Cardelli & Clayton (1991) have pointed out, lines of sight with large R_v are ideal for examining processes that modify the grain properties in dense clouds. A good correlation between the strength of the ‘2175Å’ UV bump feature and the visual extinction was also noted by Greenberg & Chlewicki (1983). Weingartner & Draine (2001a) have constructed size distributions for spherical carbonaceous and silicate grain populations in different regions of the Milky way, LMC and SMC to account for the observed near IR and microwave emission from diffuse interstellar environment using a fairly simple functional form, characterized by various parameters. They have shown that these variations can be well parameterized by R_v . Another study by Kim et al. (1994) found out that denser environments with high R_v (=5.3) have the presence of larger mean size of grains, though all denser regions may not necessarily have high R_v .

In the present study, we have used the ‘Pair method’ which is described in the section 2.1. The main purpose of the present study is to infer the size distribution, shape and composition of the interstellar dust grains, in various interstellar environments (for different values of R_v), which are consistent with the observed extinction. We use composite grain models to compare extinction toward these stars as observed by the IUE satellite. We tabulate a list of the selected stars and describe the pair method to generate the extinction curves in the UV spectral regime for these stars in section 2. DDA technique and the generation of composite grain models using it are illustrated in Section 3. In section 4, we give the results of the computed model curves and compare these model extinction curves with the observed extinction curves. In section 4, we analyze these results in detail and compare our results in terms of size and composition with those obtained by others. Our conclusions from this study are summarized in section 5.

2. PRELIMINARY DATA REDUCTION

2.1. PAIR METHOD

The standard Pair method technique is used for a set of IUE stars to generate the extinction curves. The technique involves selecting a highly reddened star and comparing it with a star (flux standard) which has negligible reddening and whose spectral features closely match with those of the reddened star. An extinction curve is then constructed by the standard relation (Massa et al. (1983)):

$$\frac{E(\lambda - V)}{E(B - V)} = \frac{m(\lambda - V) - m(\lambda - V)_o}{(B - V) - (B - V)_o} \quad (1)$$

where subscript ‘o’ refers to the unreddened star and other is for the reddened star. Here E(B-V) is the difference in extinction between the specified wavelengths and

corresponds to the color excess. The resultant extinction curve $E(\lambda - V)/E(B - V)$ is then plotted versus $1/\lambda$ for selected IUE stars.

2.2. Object Selection Criteria

We have selected 26 “program stars” (listed in Table 1) from Fitzpatrick & Massa (1988), Fitzpatrick & Massa (2009) and IUE spectral atlas by Wu et al. (1983). The R_v values of the sample reddened stars are taken from Valencic et al. (2004). The spectral types for these 26 stars lies in the range O7-B5. We have selected reddened and dereddened stars on the basis of their visible spectral type and the luminosity class. Spectral type mismatch error larger than one luminosity subclass is avoided (see Table 1) in order to account for spectral type uncertainties between reddened and the dereddened stars. Late type stars are excluded because their ultraviolet energy distributions are very strong functions of their spectral type - thus amplifying the magnitudes of error associated with the spectral mismatching between the reddened and unreddened stars. Massa et al. (1983) and Massa et al. (1984) give the identification of the features useful in matching B stars near the main sequence. Most of the sample stars are selected along different line of sights and are previously known to produce extinction curves that vary considerably from the average Milky way curve ($R_v=3.1$). The lowest value of color excess $E(B-V)$ for unreddened stars sample is 0.01 and the highest value of $E(B-V)$ for reddened stars sample is 0.95. The stars selected represent a range of environments; viz. diffuse interstellar medium (DIF); HII region (HII); OB type association (OB); reflection nebulae (RN); dense medium (DEN) and radio or HI source (H/RADIO) which are mentioned in second column of Table 1. Environment type for the stars is taken from Fitzpatrick & Massa (1988); Jenniskens & Greenberg (1993) and SIMBAD astronomical database. It is to be noted that the sample of stars selected span the value of R_v i.e the ratio of total to selective extinction, from ~ 2.0 to 5.0 (see Table 1) representing the physical environments in the galaxy i.e from a diffuse medium to a very dense medium so as to study the effects on the corresponding extinction curves. Other properties of the sample stars such as distance (in Kpc) and neutral hydrogen column densities for the sample stars chosen are given in Fitzpatrick & Massa (1990).

The column (1) of Table 1 gives the HD number of the Program star, column (2) refers to the environment type, column (3) gives HD number of comparison star followed by their visible spectral types, column (4) and (5) give magnitude in V and B band respectively, column (7) gives the color excess $E(B-V)$ values and column (8) gives the value of observed R_v .

Table 2 gives the observational data for the flux standards which are the comparison stars.

2.3. MERGING OF SPECTRAL BANDS for Pair Method

Each spectra of program star consisted of two separate images, one for the shorter wavelength and another for the longer wavelength. Data was taken from following cameras: Short Wavelength Prime (SWP, $1150\text{\AA} < \lambda < 1978\text{\AA}$), Long Wavelength Redundant (LWR, $1851\text{\AA} < \lambda < 3348\text{\AA}$) and Long Wave-

length Prime (LWP, $1851\text{\AA} < \lambda < 3347\text{\AA}$). The spectra of each reddened and unreddened star is taken from the IUE archives. For each program and the comparison star, SWP and LWR/LWP data for fluxes were merged to achieve the instrumental resolution i.e 6\AA and the resultant fluxes are converted to magnitudes $m(\lambda)$, with λ covering the wavelength range $1150\text{\AA} - 3348\text{\AA}$. The magnitudes were further interpolated in the range $1153-3201\text{\AA}$ with a binning of 1\AA . Further, extinction curves are generated using standard Pair method as discussed in Section 2.2.

3. DISCRETE DIPOLE APPROXIMATION (DDA)

An approximate technique called discrete dipole approximation (DDA) was proposed by Purcell & Pennypacker (1973). It is a powerful numerical technique for calculating the optical properties such as absorption and scattering of the target. DDA is basically designed for targets having arbitrary and irregular shape. As an approximation, the continuum target is replaced by an array of N dipoles. To each dipole, a polarizability can be assigned for a particular target composition. The polarizability depends in general on the dielectric properties such as complex refractive index $m = n + ik$ of the material inside the target. The polarizability and the refractive index of the material can be related to each other by the well known Clausius-Mossotti condition. Each dipole interacts with the neighboring dipoles on the application of electric field. After evaluating the polarization P by all the N dipoles inside the target, we can solve for the absorption and extinction cross sections of the target. The two criteria for the validity of DDA:

1) The value of $|m|kd$ should be < 1 , where m is the complex refractive index of the material, $k=2\pi/\lambda$ is the wave number in vacuum and d is the dipole spacing between the dipoles.

2) The dipole spacing d should be small enough so that the number of dipoles N should be large enough to describe the target shape satisfactorily.

For more detailed calculations, see Draine (1988). We have used discrete dipole scattering version 6.1 (DDSCAT6.1¹) for the present study. The work by Draine & Flatau (2008) may be looked upon for a more detailed analysis on the code.

3.1. Composite grain models using DDA

For this study, we have used the DDSCAT6.1 code (Draine & Flatau 2003) which has been modified and developed by Dobbie (1999) to generate the composite grain models. The code, first carves out an outer sphere (or spheroid) from a lattice of dipole sites. Sites outside the sphere are vacuum and sites inside are assigned to the host material. Once the host grain is formed, the code locates centers for internal spheres to form inclusions. The inclusions are of a single radius and their centers are chosen randomly. The code then outputs a three dimensional matrix specifying the material type at each dipole site which is then received by the DDSCAT program. In the present study the axial ratios (hereafter called AR) of the composite spheroidal grains is taken to be $AR=1.33$,

¹ <http://code.google.com/p/ddscat>

TABLE 1
EXTINCTION CURVE DETAILS FOR THE PROGRAM STARS.

HD # (Sp Type)	ENV ^a	Flux Std (Sp Type)	V	B	B-V	E(B-V)	R_v
239693 (B5 V)	DIF	25350 (B5 V)	9.54	9.77	0.23	0.41	2.37
185418 (B0.5V)	DEN	55857 (B0.5 V)	7.45	7.67	0.22	0.50	2.54
123335 (B5 IV)	HII	147394 (B5 IV)	6.31	6.37	0.06	0.24	2.60
18352 (B1 V)	DIF	31726 (B1 V)	6.80	7.03	0.23	0.47	2.66
54439 (B1.5V)	HII	74273 (B1.5V)	7.72	7.72	0.00	0.29	2.73
179406 (B3 V)	HII	190993 (B3 V)	5.33	5.46	0.13	0.35	2.73
24432 (B3 II)	HII	79447 (B3 III)	6.93	7.51	0.58	0.51	2.77
217086 (O7 V)	OB	47839 (O7 Vf)	7.65	8.28	0.63	0.95	2.80
46660 (B1 V)	HII	31726 (B1 V)	8.04	8.35	0.31	0.56	2.82
281159 (B5 V)	HI/Radio	25350 (B5 V)	8.53	9.21	0.68	0.86	2.85
21483 (B3 III)	DEN	79447 (B3 III)	7.03	7.38	0.35	0.55	2.89
53974 (B0.5IV)	RN	149881 (B0.5IV)	5.38	5.41	0.03	0.31	2.94
38131 (B0.5V)	RN	55857 (B0.5 V)	8.19	8.40	0.21	0.49	3.01
217061 (B1 V)	RN	31726 (B1 V)	8.77	9.46	0.69	0.95	3.03
205794 (B5 V)	RN	25350 (B5 V)	8.43	8.77	0.34	0.62	3.09
46202 (O9 V)	DIF	38666 (O9.5 V)	8.20	8.36	0.16	0.48	3.12
216658 (B0.5V)	RN	55857 (B0.5 V)	8.89	9.59	0.70	0.98	3.14
149452 (O9 V)	RN	214680 (O9 V)	9.07	9.65	0.58	0.84	3.37
34078 (O9.5V)	DEN	38666 (O9.5 V)	5.99	6.18	0.19	0.54	3.42
37367 (B2.5V)	DIF	37129 (B2.5 V)	5.98	6.11	0.13	0.40	3.55
252325 (B1 V)	RN	31726 (B1 V)	10.79	11.36	0.57	0.87	3.55
147701 (B5 V)	DEN	4180 (B5 III)	8.36	8.92	0.56	0.76	3.86
147889 (B2 IV)	DEN	3360 (B2 IV)	7.10	7.42	0.32	1.10	3.95
37903 (B1.5V)	RN	74273 (B1.5 V)	7.84	7.91	0.07	0.35	4.11
37061 (B1 IV)	Or N	34816 (B1 IV)	6.83	7.09	0.26	0.56	4.29
93222 (O7IIIif)	OB	47839 (O7 Vf)	8.10	8.15	0.05	0.37	4.76

^a DIF, Diffuse interstellar medium; DEN, Dense interstellar medium;

HII, HII region; OB, OB association; RN, Reflection nebula

Or N, Orion Nebula; HI/Radio source.

ENV type are taken from Fitzpatrick & Massa (1988); Jenniskens & Greenberg (1993) and SIMBAD astronomical database.

TABLE 2
OBSERVATIONAL DATA FOR FLUX STANDARD STARS

HD #	Sp type	V	B	B-V	E(B-V)
47839	O7 Vf	4.65	4.41	-0.24	0.08
214680	O9 V	4.88	4.64	-0.24	0.11
38666	O9.5 V	5.17	4.89	-0.28	0.02
55857	B0.5 V	6.11	5.85	-0.26	0.02
63922	B0 III	4.11	3.92	-0.19	0.11
149881	B0.5 IV	7.00	6.84	-0.16	0.09
75821	B0 IV	5.09	4.88	-0.21	0.08
36512	B0 V	4.62	4.36	-0.26	0.04
34816	B1 IV	4.29	4.02	-0.27	0.01
31726	B1 V	6.15	5.94	-0.21	0.05
74273	B1.5 V	5.87	5.69	-0.18	0.03
3360	B2 IV	3.66	3.46	-0.20	0.04
37129	B2.5 V	7.13	6.99	-0.14	0.07
79447	B3 III	3.96	3.77	-0.19	0.01
190993	B3 V	5.07	4.89	-0.18	0.02
147394	B5 IV	3.90	3.75	-0.15	0.01
25350	B5 V	5.28	5.13	-0.15	0.01

2.0 and 1.44 with number of dipoles $N=9640$, 14440 and 25896 respectively. The dipole sites are either silicates, graphites or vacuum. The optical constants of silicates and graphites are taken from Draine & Anderson (1985) and Draine (1987). The spheroidal composite grain consists of silicates as the host and graphites as the inclusion. In order to study the effect of volume fraction of graphite inclusion, we use three different volume fraction ‘ f ’ of graphite grain inclusion viz. $f=0.1$, 0.2 and 0.3.

Table 3 shows the number of dipoles for each grain

model along with the axial ratio and number of dipoles per inclusion with the number of inclusions for each fraction. The calculations of extinction cross sections of the target depend in general upon the orientation of the target. Hence, we average over 27 orientations of the target for all the calculations done by DDA. For more details on the composite grain models and the modified code see Vaidya et al. (2007).

Fig. 1 illustrates a composite grain model with $N=9640$ dipoles composed of silicates as host (in green)

TABLE 3
 NUMBER OF DIPOLES FOR EACH INCLUSION OF THE GRAIN MODEL
 ALONG WITH AXES LENGTHS FOR SPHEROID IN X,Y,Z DIRECTION
 FOR HOST (H) AND INCLUSION (I). ALSO, NUMBER OF INCLUSIONS
 IS MENTIONED IN BRACKETS IN COLUMN 3,4 & 5 FOR EACH OF THE
 VOLUME FRACTION f OF INCLUSIONS.

N (AR)	$N_x/N_y/N_z$	No. of dipoles per inclusion (No. of inclusions)		
		$f=0.1$	$f=0.2$	$f=0.3$
9640(1.33)	H:32/24/24 I: 8/6/6	152(6)	152(11)	152(16)
25896(1.50)	H:48/32/32 I:12/8/8	432(7)	432(13)	432(19)
14440(2.00)	H:48/24/24 I:12/6/6	224(6)	224(11)	224(16)

and graphite as inclusion (in red). The inclusions can be seen clearly in Fig. 2. There are eleven such inclusions consisting of 152 dipoles per inclusion. This model represents a composite dust grain with volume fraction of graphite $f = 0.2$.

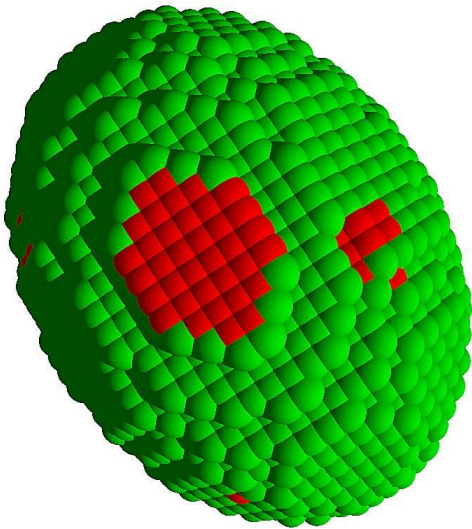


FIG. 1.— A non-spherical composite dust grain consisting of host (in green) and inclusion (in red) with a total of $N=9640$ dipoles where the inclusions embedded in the host spheroid are shown such that only the ones placed at the outer periphery are seen.

4. RESULTS AND DISCUSSIONS

The following are the principal results of this work:

4.1. Extinction efficiencies of the composite grain

Though the exact composition of the interstellar dust is still uncertain, graphites and silicates are the most often used for cosmic dust models (see for example Mathis et al. (1977); Draine & Lee (1984)). We have checked the extinction of graphite and amorphous carbon (AMC) as possible candidates for explaining the UV feature at 2175\AA . Figure 3 shows the extinction curve for very small AMC and graphite grain of radius $a=0.01\mu\text{m}$. It is seen that the AMC does not show any

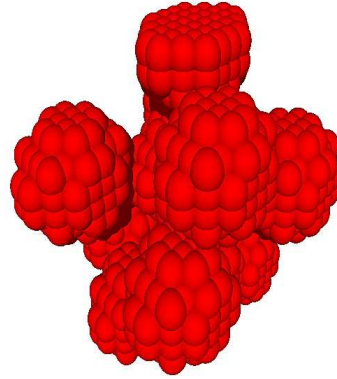


FIG. 2.— This figure shows the inclusions of the composite grain. The volume fraction f of graphite inclusions is 0.2. The number of inclusions are 11 with 152 dipoles per inclusions.

peak at 2175\AA , whereas graphite prominently shows this feature. Amorphous carbon is also highly absorbing at very long wavelengths and would provide most of the extinction longward of $0.3\mu\text{m}$ ($3.3\mu\text{m}^{-1}$) as seen by Draine (1989) and Weingartner & Draine (2001b). Grain models with AMC are also not favored by Zubko et al. (2004b). Instead, large polycyclic aromatic hydrocarbons (PAHs) molecules are likely candidates as carriers of the 2175\AA feature – a natural extension of the graphite hypothesis (Joblin et al. 1992; Li & Draine 2001). Clayton et al. (2003a) have also considered PAHs as one of the constituents in the dust model to explain the interstellar extinction in the UV.

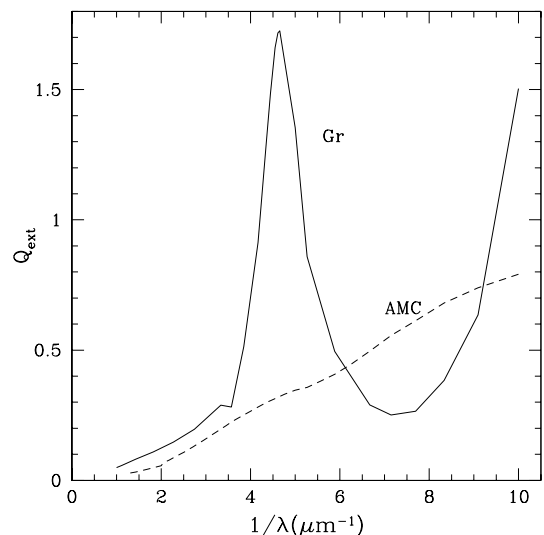


FIG. 3.— Extinction efficiencies for amorphous carbon (AMC) and graphite grains for very small grain size of $0.01\mu\text{m}$ is shown in this figure. The peak in graphite curve at spectral wavelength 2175\AA explains why it is being used as inclusion in our composite grain model whereas no such peak is seen in AMC curve at 2175\AA .

We calculate the extinction efficiencies Q_{ext} for a composite grain model consisting of a host silicate spheroid along with graphite inclusions with the number of dipoles being $N = 9640, 14440$ and 25896 . The extinction efficiencies are calculated for target which are prolate spheroid in our case. The volume fractions, f of the graphite inclusions in the composite grain is varied as $f=0.1, 0.2$ and 0.3 . The extinction efficiencies for the composite grain model having number of dipoles $N = 9640$ ($AR = 1.33$) with the variation in the volume fraction of graphite inclusion are shown in Fig. 4. The variation of extinction efficiencies for the composite grain model of the number of dipoles $N = 14440$ ($AR = 2.0$) and $N = 25896$ ($AR = 1.50$) with the variation in the volume fraction of graphitic inclusions can be seen in Fig. 5 and 6 respectively. It is clearly noted that the extinction efficiencies and the shape of the extinction curves vary considerably as the grain size increases. The 2175\AA feature is clearly seen for small grains, viz. $a=0.01\mu m$ and $0.05\mu m$, whereas for the larger sizes ($a=0.1\mu m$ and $0.2\mu m$), the feature disappears. For both the models, we see a shift in the peak wavelength at 2175\AA as the volume fraction of the inclusion increases. Further, the extinction efficiency is seen to vary with the variation in the volume fraction of graphite inclusion.

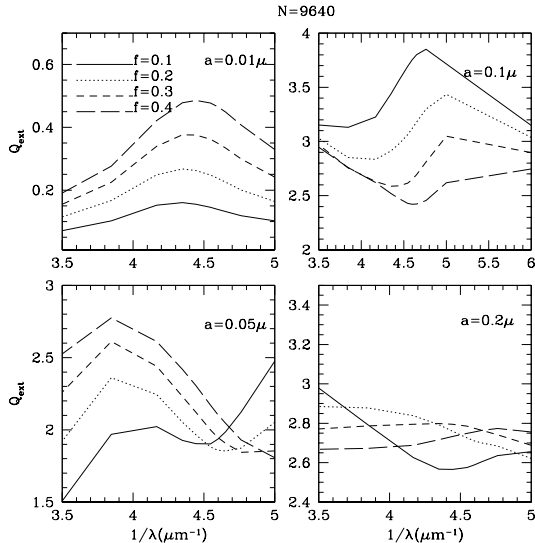


FIG. 4.— The figure shows extinction efficiencies for a composite grain model with number of dipoles, $N = 9640$ for volume fractions of graphite inclusions, $f=0.1, 0.2, 0.3$ and 0.4 . These extinction curves clearly show a shift in the peak wavelength ‘ 2175\AA ’ ($4.57\mu m^{-1}$) and variation in extinction efficiency as the volume fraction of graphite varies. It is also to be noted that the ‘ 2175\AA ’ feature vanishes for large grains with $a=0.2\mu m$

4.2. Interstellar extinction curve

The interstellar extinction curve (i.e. the variation of the extinction with wavelength) is usually expressed by the ratio: $E(\lambda-V)/E(B-V)$ vs $1/\lambda$. A power law for the grain size distribution, $n(a) \sim a^{-3.5}$ (Mathis et al. 1977); where $a_{min} < a < a_{max}$ is used for evaluating the interstellar extinction curve for a given grain size distribution. We calculate the extinction efficiencies of the grain models using the above power law. It must be noted that

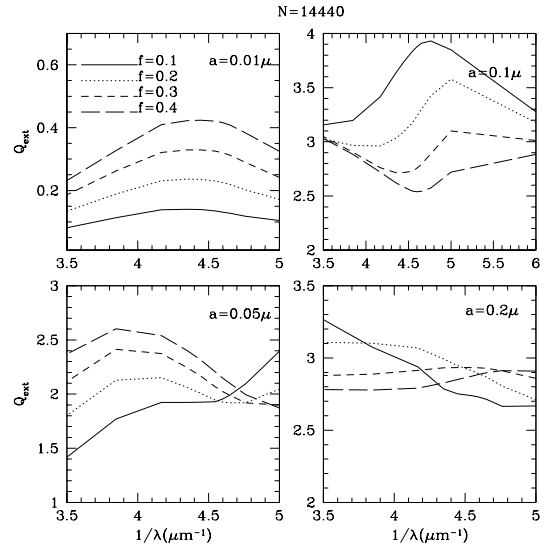


FIG. 5.— The figure shows extinction efficiencies for a composite grain model with number of dipoles $N = 14440$. The shift in the peak wavelength and variation in extinction efficiency with the volume fraction variation of graphite is seen.

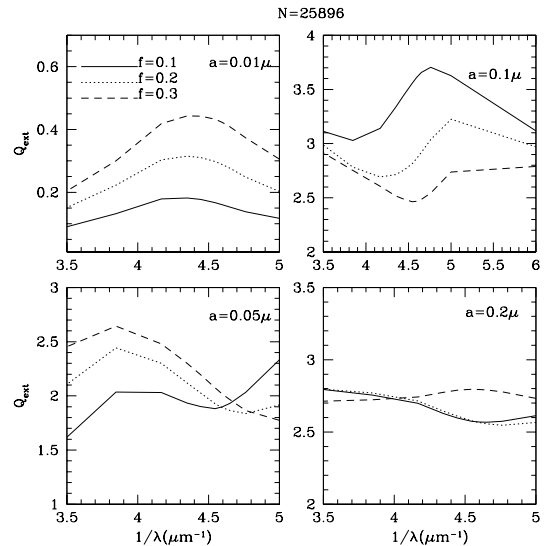


FIG. 6.— In this figure, the extinction efficiencies for a composite grain model with number of dipoles $N = 25896$ and volume fraction of graphite $f = 0.1, 0.2$ and 0.3 is shown. A shift in the peak wavelength and variation in extinction efficiency as the volume fraction of graphite varies is seen.

we have used two types of size distribution (i) $a=0.001-0.100\mu m$ (denoted as a_{100} henceforth) and (ii) $a=0.005-0.250\mu m$ (denoted as a_{250} henceforth). Earlier, we have used the porous (Vaidya & Gupta 1997, 1999) and the composite spheroidal grain models (Vaidya et al. 2007) to interpret the average observed extinction curve in the wavelength range $0.1\mu m-3.4\mu m$ (Vaidya et al. 2007). In this paper, we use the composite spheroidal grain models to interpret the observed extinction in the UV, in several directions towards individual stars, selected from various galactic environments (Fitzpatrick & Massa 1990; Valencic et al. 2004). Subsequently, in case of composite grain models, each interstellar extinction curve of the observed IUE star is compared with the model curve formed

from a χ^2 minimized and best fit linear combination of the composite grains (contributory fraction p) and solid graphite grains (contributory fraction q). By varying p and q each from 0.1 to 1.0 in steps of 0.1, a set of 20 model curves are generated and on comparing these model curves with the observed extinction curve of the stars, a set of reduced χ^2 are obtained. A minimum χ^2 from this set is chosen depending on the linear combination of p and q . Hence, we obtain a net model interstellar extinction curve as a result of the linear combination of p and q which gives a minimum χ^2 value. We use the following formula to obtain the set of reduced χ^2 (Bevington 1969):

$$\chi_j^2 = \frac{\sum_{i=1}^n (S_i^j - T_i^k)^2}{pp}$$

where pp is the number of degrees of freedom, $S_i^j(\lambda_i)$ is the j th model curve for the corresponding p and q linear combination of the composite grains and bare graphite grains and $T_i^k(\lambda_i)$ is for the observed curve, λ_i are the wavelength points with $i=1, n$ for $n=12$ wavelength points of the extinction curves.

Tables 4 shows the best fit parameters along with the minimized χ^2 values for the composite grain model using DDA for 26 IUE stars.

Fig. 7 and 8 shows the comparison of the observed interstellar extinction curve with the best fit model for composite grains generated using DDA technique. From Table 1 & 4 it is seen that the grain models with the size distribution $a=0.001-0.100 \mu m$ fit the observed extinction curves towards stars with low R_v (2-3), whereas, stars with high R_v (4-6) fit the grains with the sizes distribution, $a= 0.005-0.250 \mu m$.

Our results on the composite spheroidal grain models i.e Table 4, Fig 7 and 8 show the best fit parameters; size distributions $0.001-0.1 \mu m$ ($a100$) and $0.005-0.250 \mu m$ ($a250$), shape-axial ratio; 1.33-2.0 and the composition-volume fraction of the graphite inclusions $f = 0.1, 0.2$ and 0.3 ; for the grains in the interstellar medium towards the 26 selected stars as observed by the IUE satellite.

4.3. Environmental effects

In order to examine how the extinction properties are influenced by the various dust environments, we have analyzed the extinction curves for stars in seven different galactic environments; as shown in Table 1. The variation in the strength and width of the 2175Å feature is seen for various environments i.e. from dense regions and reflection nebulae to diffuse clouds (Fig. 7 and 8). It can be clearly seen that the dust in the dense quiescent environments and reflection nebulae produces broad bumps of larger widths whereas those stars lying in the diffuse environment produces narrower bumps of average widths. Stars around HII regions and/or which are a part of OB association produces bump of average widths with weak bumps. This results are in accordance with Fitzpatrick & Massa (1986). They have shown that the observed width of the bump is strongly subject to environmental influences by calculating the widths of the bump and the area under the bump through the analytic parameterization scheme.

In Fig. 7 and 8, we show the fitting of the extinction curves for stars in the HII region (HII), reflection nebula

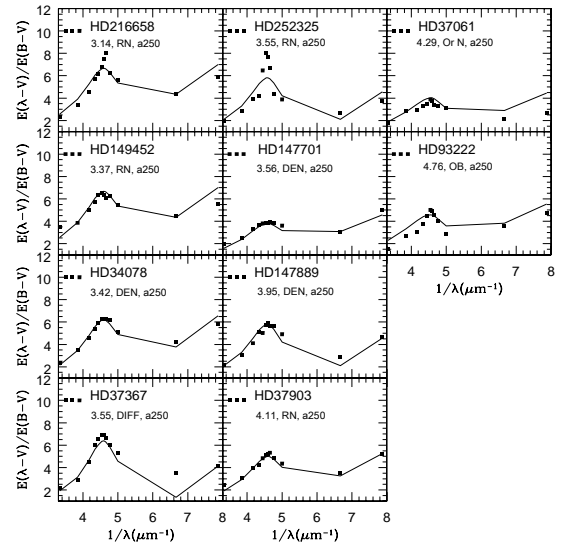


FIG. 7.— Comparison of the observed interstellar extinction curves with the best fit composite grain model extinction curves (generated using DDA) in the wavelength range $3.17-7.87 \mu m^{-1}$ ($3200-1200\text{\AA}$). The observed R_v , environment type and the best fit grain size distribution for the sample is mentioned inside the figure.

(RN) and dense medium (DEN + DC) with our models. The ratio, R_v also varies from 2.37 for HD239693 to 4.76 for HD93222. These curves further highlight star to star variation in the extinction, demonstrating the sensitivity to local conditions. In particular, a large variation in the strength and width of the 2175Å feature is seen in the extinction curves for the stars lying in the dense region i.e HD37903 ($R_v=4.11$), HD37061 ($R_v=4.29$) and HD93222 ($R_v=4.76$). The shape of the extinction curves for the stars in the HII region (Fig. 7 and 8) shows variation in the spectral region, shortward of 1500\AA . In particular, see the steep rise in the extinction for HD24432 ($R_v=2.77$). This star lying in the diffuse clouds is fitted by the composite dust grain model of $N=9640$ with $a100$ size distribution. Thus, each extinction curve contains unique information about the grains along its sight line. Using analytic parameterization method, Fitzpatrick and Massa (1986, 1988) have also shown that the observed width of the 2175Å feature is strongly subject to the environmental influences.

Our results on the composite grains show that the parameter R_v varies from ~ 2 for small grains ($a=0.01 \mu m$) to ~ 5 for the larger grains ($a=0.2 \mu m$). These results also show consistency for the denser medium where R_v has a small value (presence of small grains) and for the diffuse regions where R_v has high value (presence of

TABLE 4
BEST FIT χ^2 VALUES AND OTHER PARAMETERS FOR DIFFERENT COMPOSITE GRAIN MODELS GENERATED USING DDA TECHNIQUE.

HD #	χ^2	p	q	N	f_{Gr}	$a(\mu m)$
239693	0.1552	0.2	0.4	14440	0.1	0.001-0.100
185418	0.2032	0.1	0.6	14440	0.2	0.001-0.100
123335	0.3719	0.2	0.4	14440	0.1	0.005-0.250
18352	0.0535	0.2	0.5	14440	0.1	0.005-0.250
54439	0.4001	0.1	0.4	9640	0.1	0.001-0.100
179406	0.2239	0.3	0.3	14440	0.1	0.001-0.100
24432	0.3149	0.4	0.4	9640	0.1	0.001-0.100
217086	0.1722	0.2	0.4	14440	0.1	0.001-0.100
46660	0.1488	0.1	0.5	14440	0.1	0.001-0.100
281159	0.1477	0.2	0.4	14440	0.1	0.001-0.100
21483	0.1714	0.3	0.3	9640	0.1	0.001-0.100
53974	0.0963	0.2	0.3	9640	0.1	0.005-0.250
38131	0.2747	0.5	0.3	14440	0.1	0.005-0.250
217061	0.0552	0.2	0.4	14440	0.1	0.005-0.250
205794	0.1625	0.1	0.4	9640	0.1	0.005-0.250
46202	0.2304	0.4	0.4	14440	0.1	0.005-0.250
216658	0.2200	0.4	0.4	14440	0.1	0.005-0.250
149452	0.0778	0.4	0.4	14440	0.1	0.005-0.250
34078	0.0920	0.3	0.4	14440	0.1	0.005-0.250
37367	0.1760	0.1	0.5	14440	0.1	0.005-0.250
252325	0.2172	0.2	0.4	14440	0.3	0.005-0.250
147701	0.0926	0.3	0.2	9640	0.1	0.005-0.250
147889	0.0652	0.2	0.4	14440	0.3	0.005-0.250
37903	0.0852	0.3	0.3	14440	0.1	0.005-0.250
37061	0.1372	0.2	0.2	14440	0.3	0.005-0.250
93222	0.0969	0.3	0.2	14440	0.3	0.005-0.250

larger grains). These results are also consistent with the strength of the 2175Å feature viz., for the larger grains ($a=0.2\mu m$), the feature is suppressed. See for example, Fig. 7 in Vaidya et al. (2007).

We would like to discuss here a distinct contribution of the type of media to the spectral band feature viz., the bump at 2175Å. We have seen that contribution to this bump feature is due to the presence of very small graphite grains. The size of the grain shows a tremendous effect on the extinction cross sections. Hence, weakening of the bump feature can be attributed to the removal of very small grains from the dust population of the media for example; clumpy media and those of unresolved sources which are classified as extended and inhomogeneous media. Using effective medium theory (Bruggeman mixing rule), Kruegel & Siebenmorgen (1994) have shown variation in 2175Å bump feature and flattening of UV extinction curve for fluffy dust aggregates of silicate, carbon and ice with increasing grain sizes.

Extinction measured for an region is directly related to the optical depth along the line of sight. For few of the sample stars with clumpy and dense molecular media, a weakening of 2175Å peak along with flattening of extinction curve is seen. This effect is attributed to the influence of scattering on the extinction properties, specially the bump feature, of the stars. Natta & Panagia (1984) have observed a suppression in the 2175Å peak followed by a flattening of far UV curve, with increasing optical depth of the media. They have also shown that inhomogeneous layer of high optical depth (high R_v) tends to produce gray extinction.

Similar studies for low optical media have been conducted by Krügel (2009). They have investigated the influence of scattering on the extinction curve of stars. They have computed effective optical depth τ_{eff} for a variety of idealized geometrical configurations (spheres, slabs and blocks) for varying optical depth τ and analyzed the dependencies of effective optical thickness τ_{eff} on the various measurable optical properties of the dust including τ . They also found out that standard dust is sensitive to spatial resolution and the structure of the medium (clumpiness, foreground/background). The extinction cross sections calculated by them, taking into account the scattering effects, for clumpy, homogeneous media and spatially unresolved stars show marked differences to the standard reddening curve.

Mathis & Whiffen (1989) have fitted certain sight lines ($R_v=3.02, 4.83$) using effective medium approximation (Bruggeman mixing rule). They used composite grains (silicates and amorphous carbon) and obtained large size grains as the best fit parameter for sight lines with higher R_v values. Wolff et al. (1993) have used composite grains to model interstellar polarization towards eight lines of sight. They have used DDA to model the composite grains. However, their composite grain model with silicates and amorphous carbon/ organic refractory material failed to reproduce the observed polarization curve.

Several other groups have presented studies on size and composition of dust grains in interstellar medium using various techniques. For example, Zubko et al. (2004b) have presented a dust model consisting of various components: PAH's, bare silicates & AMC as well as compos-

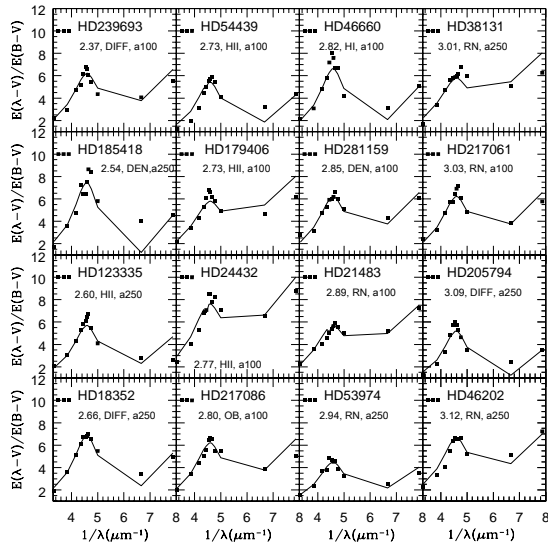


FIG. 8.— Comparison of the observed interstellar extinction curves with the best fit composite grain model extinction curves (generated using DDA) in the wavelength range $3.17\text{--}7.87\ \mu\text{m}^{-1}$ ($3200\text{--}1200\ \text{\AA}$). The observed R_v , environment type and the best fit grain size distribution for the sample is mentioned inside the figure.

ite particles containing silicate, organic refractory material, water ice and voids. They have used the method of regularization (MR) to solve for the optimal grain size distribution of each dust component knowing the observational constraints and the dust constituents and properties. Clayton et al. (2003a) have employed a modified version of the MEM fitting algorithm, developed by Kim et al. (1994) to fit the observed extinction in eight preferred sightlines/directions. They have used a 3-component homogeneous spherical grain model consisting of silicates, graphite and AMC as well as composite grain model consisting of pyroxenes, AMC and vacuum. Clayton et al. (2003a) adopted solar abundances and used EMT (extension of Bruggeman rule) to compute the optical constants of composite grains. With the 3-component homogeneous grain, they obtained the upper size cutoffs of $0.3\ \mu\text{m}$ for graphite and AMC and $1\ \mu\text{m}$ for silicate grains. With the composite grain models, Clayton et al. (2003a) obtained the fit to the average observed galactic extinction curve with 0.80 (Solar) Si (Pyroxene) and 0.36 (Solar) C abundance and found the upper size cutoff size for composite grain to be $1\ \mu\text{m}$. Clearly, both these grain models of Clayton et al. (2003a) show deficit of small silicate and graphite grains. On the other hand, we have found all the fits with smaller size cutoffs of $0.100\ \mu\text{m}$ and $0.250\ \mu\text{m}$ as compared to size cutoffs of Clayton et al. (2003a). Although

Clayton et al. (2003b) have used AMC as a third component, we did not use it since AMC exhibits absorption at about $2500\ \text{\AA}$. It is also highly absorbing at very long wavelengths and thus would provide most of the extinction longword of $0.3\ \mu\text{m}$ (Draine 1989). Recently, Gordon et al. (2009) have analyzed FUSE+IUE extinction curves for 75 sightlines and have compared these curves with three different dust grain models given by Weingartner & Draine (2001b); Clayton et al. (2003b) and Zubko et al. (2004b). Gordon et al. (2009) found that the models of Clayton et al. (2003b) and Zubko et al. (2004b) provide much better fits than Weingartner & Draine (2001b) model.

It is clear that the variation in the grain size distribution subject to the variation in the environment indicates that the small sized grains coagulate onto large grains in relatively dense environments, as expected (Draine 1985, 1990). Mathis & Whiffen (1989) have fitted certain sight lines ($R_v=3.02, 4.83$) using effective medium approximation (Bruggeman mixing rule). They used composite grains (silicates and amorphous carbon) and obtained large size grains as the best fit parameter for sight lines with higher R_v values. Weingartner & Draine (2001a) have fitted a specific case of extinction toward HD21021 with small value of $R_v=2.1$ with a small grain size distribution of graphite/silicate grains using a simple functional fitting form.

Shape of the grain is an important factor in determining the interstellar extinction. Gupta et al. (2005) have calculated the extinction efficiency for various shapes of silicate and graphitic spheroidal grains such as oblates, prolates and spheres using T-matrix theory. They have very well described the considerable variation in the extinction due to the different axial ratio grains as compared to the simple case of sphere. They also find out the best fit for explaining the observed extinction is obtained with a grain size distribution $a=0.005\text{--}0.250\ \mu\text{m}$ having an axial ratio of $AR=1.33$. However, in this work, we have used a more realistic composite dust grain model generated using DDA. We find out that most of the observed directions are well fitted by axial ratio (AR) equal to 2.0. Hence, we conclude that shape of the grain has an important role in determining the observed extinction properties of stars observed by IUE satellite.

The composite grain models with silicate as host material and graphite inclusions, presented in this study is found to fit the observed extinction curves towards the stars lying in various interstellar environments. It must also be emphasized here that we have used more realistic DDA method to calculate the extinction efficiencies for the spheroidal composite grains. It must also be noted that Perrin & Lamy (1990); Perrin & Sivan (1990), Wolff et al. (1994, 1998), Vaidya et al. (2007) and Vaidya & Gupta (2011) have shown that DDA is more accurate than the EMT based grain models.

We plan to use the composite grain model with other carbonaceous materials as inclusions such as PAHs or SiC (Weingartner & Draine 2001b; Clayton et al. 2003a) for obtaining better fits in the UV region, $1500\ \text{\AA}\text{--}1200\ \text{\AA}$. We also plan to interpret the extinction towards some more stars observed by the IUE satellite.

5. CONCLUSIONS

We have used more realistic DDA method to calculate the extinction efficiencies of the spheroidal composite grains made up of the host silicate and graphite inclusions in the wavelength region of 1200Å -3200Å . We have then, used the extinction efficiencies of the composite grains for a power law size distribution (Mathis et al. 1977) to evaluate the interstellar extinction curves in the wavelength range 1200Å -3200Å . In the present study, we have used two size distributions viz. (i) $a=0.001-0.100 \mu m$ and (ii) $a=0.005-0.250 \mu m$. These extinction curves for the spheroidal composite grains are compared with the observed extinction curves obtained from the IUE satellite data to infer the parameters such as size, shape and composition of grains. The important implications of the obtained results in terms of these physical parameters (as compared to the earlier studies) are discussed in the previous section. This study made use of a more sophisticated technique for modeling a composite dust model with various parameters that are able to characterize the actual physical dust parameters for a sample of stars, lying in different interstellar environments. The main conclusions of our study are as follows:

(i) The extinction properties of the composite grains vary considerably with the variation in the volume fraction of the inclusions. In particular, the extinction peak at '2175Å ' shifts and broadens with variation in the graphite inclusions.

(ii) The composite spheroidal grain models, with axial ratios 1.33 and 2.0 and volume fraction of inclusions $f = 0.1 - 0.3$, fit the observed extinction curves reasonably well.

(iii) The ratio $R_v = A(V)/E(B - V)$ is seen to be well correlated with the '2175Å ' feature. From the sample

of 26 IUE stars, those lying in the dense regions with high R_v (4-5), show a weakening of the bump feature at 2175Å followed by a flattening of far UV extinction curve whereas stars in the diffuse interstellar medium with low R_v (2-3) show a distinct bump at this particular wavelength. This study clearly indicates, how the extinction properties of the grains vary with the optical depth of the media (which is related to R_v) and also the grain size. It is to be noted that scattering off many unresolved stellar sources also flattens the extinction curve at this wavelength.

These results are consistent as suggested earlier by Natta & Panagia (1984), Kruegel & Siebenmorgen (1994) and Krügel (2009).

In this study, we have presented the composite grain model, consisting of host silicate and graphite as inclusions and have used the results obtained for these composite grain model to infer the size distributions, shape of the grain and volume fraction of the graphite inclusions, of the interstellar dust towards 26 stars situated in the various interstellar environments. Further the composite grain models, presented in this paper, simultaneously explain the observed interstellar extinction (Vaidya et al. 2001, 2007), infrared emission from the circumstellar dust (Vaidya & Gupta 2011), scattering by the cometary dust (Gupta et al. 2006) and cosmic abundances (Vaidya et al. 2007).

6. ACKNOWLEDGMENTS

The authors acknowledge the ISRO-RESPOND project (No. ISRO/RES/2/2007-08) for funding this research.

REFERENCES

- Aiello, S., Barsella, B., Chlewicki, G., Greenberg, J. M., Patriarchi, P., & Perinotto, M. 1988, in ESA Special Publication, Vol. 281, ESA Special Publication, 223–226
- Bevington, P. R. 1969, Data reduction and error analysis for the physical sciences, ed. Bevington, P. R.
- Brownlee, D. E. in , Astrophysics and Space Science Library, Vol. 134, Interstellar Processes, ed. D. J. Hollenbach & H. A. Thronson, Jr., 513–530
- Cardelli, J. A. & Clayton, G. C. 1991, AJ, 101, 1021
- Cardelli, J. A., Clayton, G. C., & Mathis, J. S. 1989, ApJ, 345, 245
- Clayton, G. C., Gordon, K. D., Salama, F., Allamandola, L. J., Martin, P. G., Snow, T. P., Whittet, D. C. B., Witt, A. N., & Wolff, M. J. 2003a, ApJ, 592, 947
- Clayton, G. C. & Mathis, J. S. 1988, ApJ, 327, 911
- Clayton, G. C., Wolff, M. J., Sofia, U. J., Gordon, K. D., & Misselt, K. A. 2003b, ApJ, 588, 871
- Dobbie, J. 1999, PhD. Thesis, Dalhousie University
- Draine, B. 1989, in IAU Symposium, Vol. 135, Interstellar Dust, ed. L. J. Allamandola & A. G. G. M. Tielens, 313–+
- Draine, B. T. in , Protostars and Planets II, ed. D. C. Black & M. S. Matthews, 621–640
- Draine, B. T. 1987, ApJS, 64, 505
- 1988, ApJ, 333, 848
- Draine, B. T. 1990, in Astronomical Society of the Pacific Conference Series, Vol. 12, The Evolution of the Interstellar Medium, ed. L. Blitz, 193–205
- Draine, B. T. & Anderson, N. 1985, ApJ, 292, 494
- Draine, B. T. & Flatau, P. J. 2003, ArXiv Astrophysics e-prints
- 2008, ArXiv e-prints
- Draine, B. T. & Lee, H. M. 1984, ApJ, 285, 89
- Draine, B. T. & Malhotra, S. 1993, ApJ, 414, 632
- Dwek, E. 1997, ApJ, 484, 779
- Fitzpatrick, E. L. & Massa, D. 1986, ApJ, 307, 286
- 1988, ApJ, 328, 734
- 1990, ApJS, 72, 163
- 2009, ApJ, 699, 1209
- Gordon, K. D., Cartledge, S., & Clayton, G. C. 2009, ApJ, 705, 1320
- Greenberg, J. M. & Chlewicki, G. 1983, ApJ, 272, 563
- Gupta, R., Mukai, T., Vaidya, D. B., Sen, A. K., & Okada, Y. 2005, A&A, 441, 555
- Gupta, R., Vaidya, D. B., Bobbie, J. S., & Chylek, P. 2006, Ap&SS, 301, 21
- Iati, M. A., Giusto, A., Saija, R., Borghese, F., Denti, P., Cecchi-Pestellini, C., & Aiello, S. 2004, ApJ, 615, 286
- Jenniskens, P. & Greenberg, J. M. 1993, A&A, 274, 439
- Joblin, C., Leger, A., & Martin, P. 1992, ApJ, 393, L79
- Katyal, N., Gupta, R., & Vaidya, D. B. 2011, Earth, Planets, and Space, 63, 1041
- Kim, S., Martin, P. G., & Hendry, P. D. 1994, ApJ, 422, 164
- Kruegel, E. & Siebenmorgen, R. 1994, A&A, 288, 929
- Krügel, E. 2009, A&A, 493, 385
- Li, A. & Draine, B. T. 2001, in Bulletin of the American Astronomical Society, Vol. 33, American Astronomical Society Meeting Abstracts, 1451
- Li, A. & Greenberg, J. M. 1998, A&A, 331, 291
- Mallocci, G., Mulas, G., Cecchi-Pestellini, C., & Joblin, C. 2008, A&A, 489, 1183
- Massa, D., Savage, B. D., & Cassinelli, J. P. 1984, ApJ, 287, 814
- Massa, D., Savage, B. D., & Fitzpatrick, E. L. 1983, ApJ, 266, 662
- Mathis, J. S. 1996, ApJ, 472, 643
- Mathis, J. S., Rumpl, W., & Nordsieck, K. H. 1977, ApJ, 217, 425
- Mathis, J. S. & Whiffen, G. 1989, ApJ, 341, 808
- Meyer, D. M. & Savage, B. D. 1981, ApJ, 248, 545
- Natta, A. & Panagia, N. 1984, ApJ, 287, 228
- Ossenkopf, V. 1991, A&A, 251, 210
- Perrin, J. & Lamy, P. L. 1990, ApJ, 364, 146
- Perrin, J. & Sivan, J. 1990, A&A, 228, 238
- Purcell, E. M. & Pennypacker, C. R. 1973, ApJ, 186, 705
- Siebenmorgen, R., Voshchinnikov, N. V., & Bagnulo, S. 2013, ArXiv e-prints
- Stecher, T. P. 1965, ApJ, 142, 1683
- 1969, ApJ, 157, L125+
- Stecher, T. P. & Donn, B. 1965, ApJ, 142, 1681

- Vaidya, D. B. & Gupta, R. 1997, *A&A*, 328, 634
—, 1999, *A&A*, 348, 594
—, 2011, *A&A*, 528, A57+
- Vaidya, D. B., Gupta, R., Dobbie, J. S., & Chylek, P. 2001, *A&A*, 375, 584
- Vaidya, D. B., Gupta, R., & Snow, T. P. 2007, *MNRAS*, 379, 791
- Valencic, L. A., Clayton, G. C., & Gordon, K. D. 2004, *ApJ*, 616, 912
- Voshchinnikov, N. V. & Henning, T. 2008, *A&A*, 483, L9
- Voshchinnikov, N. V., Il'in, V. B., Henning, T., & Dubkova, D. N. 2006, *A&A*, 445, 167
- Weingartner, J. C. & Draine, B. T. 2001a, *Apj*, 548, 296
—, 2001b, *ApJ*, 548, 296
- Wolff, M. J., Clayton, G. C., & Gibson, S. J. 1998, *ApJ*, 503, 815
- Wolff, M. J., Clayton, G. C., Martin, P. G., & Schulte-Ladbeck, R. E. 1994, *ApJ*, 423, 412
- Wolff, M. J., Clayton, G. C., & Meade, M. R. 1993, *ApJ*, 403, 722
- Wu, C., Ake, T. B., Boggess, A., Bohlin, R. C., Imhoff, C. L., Holm, A. V., Levay, Z. G., Panek, R. J., Schiffer, III, F. H., & Turnrose, B. E. 1983, *NASA IUE Newsl.*, No. 22, 2+324 pp., 22
- Xiang, F. Y., Li, A., & Zhong, J. X. 2011, *ApJ*, 733, 91
- Zubko, V., Dwek, E., & Arendt, R. G. 2004a, *ApJS*, 152, 211
—, 2004b, *ApJS*, 152, 211